McsB Is a Protein Arginine Kinase That Phosphorylates and Inhibits the Heat-Shock Regulator CtsR

Jakob Fuhrmann *et al.*

Science **324**, 1323 (2009);
DOI: 10.1126/science.1170088

Science (print ISSN 0036-8075; online ISSN 1095-9203) is published weekly, except the last week in December, by the American Association for the Advancement of Science, 1200 New York Avenue NW, Washington, DC 20005.

the profile from *Hoxd9* to *Hoxd1* was comparable to wild type. The robust gain in H3K4me3 marks over *Hoxd12* was not scored in older wild-type tail buds (fig. S2) and did not match any transcriptional activity, neither for *Hoxd12* nor for *Hoxd11* (Fig. 3B). In this case, both *Hoxd11* and *Hoxd12* were ready to be transcribed (*28*), yet they remained silent because they were moved away from the required enhancer sequence located telomeric to the breakpoint. In contrast, increased H3K4 trimethylation on the other side of the breakpoint (Fig. 3C) matched the premature activation of *Hoxd10*.

The DNA interval decorated by H3K27me3 marks in *inv* mutants was virtually identical to wild type (Fig. 3C), indicating that an integral cluster is not necessary to define the initial extent of the repressive domain; H3K27me3 marks were positioned over posterior genes even though these genes were disconnected from the rest of the cluster, thus ruling out the existence of a spreading mechanism sensu stricto for the implementation of this repression. In addition, the overall density of these marks on both sides of the break point was considerably below the wild-type situation (Fig. 3C). In the posterior half-cluster, H3K27me3 marks were distributed almost as in wild type over *Evx2* and *Hoxd13*, whereas a decrease was scored over the *Hoxd12* to *Hoxd11* intergenic region and 3′ to *Hoxd11* (Fig. 3C). In the anterior half-cluster, a similar reduction was detected at the *Hoxd10* locus, consistent with its premature activation and, to a lesser extent, over *Hoxd9* (Fig. 3C). This weakening in H3K27me3 signal over *Hoxd10* was not observed at the wild-type locus, even in older tail buds (fig. S2). The general decrease in H3K27 trimethylation around the break point suggests that a dense coverage of the *HoxD* cluster by this histone modification requires an intact clustered configuration. Whereas isolated parts of the gene cluster can be trimethylated at H3K27 independently of one another, these various parts may cooperate and synergize to mediate a dense pattern of methylation, potentially through local cis interactions.

These results shed light on the general regulatory strategy implemented by *Hox* gene loci during the earliest steps of mouse trunk development. Unlike in *Drosophila*, mammalian *Hox* gene loci appear refractory to transcription before transcription initiates, as indicated by high levels of H3K27me3 marks covering the *HoxD* locus early on. This likely reflects the necessity to prevent the premature activation of posterior genes at a time when anterior structures are being determined, which would be deleterious to the embryo. During gastrulation, this repression is counteracted by an activity progressing from the telomeric to the centromeric extremity of the cluster, illustrated by both an elevation of H3K4me3 level and the demethylation of H3K27me3. The region of transition between these two states of chromatin corresponds to the dynamic window wherein *Hoxd* genes become transcriptionally active. Alternatively, *Hox* genes could be activated from a persisting pool of nonexpressing stem cells. In this view, the chromatin modifications observed in our samples reflect the average of successive waves of transcriptional activation rather than a dynamic process occurring in the same cells. We do not favor this possibility because such a pool of *Hox*-negative cells would constitute a large fraction of the tissue sample, yet it has never been observed in gastrulating tail buds. Also, the nucleosomes of these stem cells would lack the repressive marks over the *HoxD* cluster, unlike in ESC. Finally, *Hox* genes are activated in cells already expressing more anterior combinations thereof.

We have shown that gene clustering is not necessary for the initial definition of the H3K27me3 landscape. However, clustering is required for a full repression to be consolidated and/or maintained over the cluster, which suggests a synergistic effect due to *Hox* genes' density. Likewise, whereas an integral cluster appears dispensable for selecting the sites of H3K4 trimethylation, gene clustering helps the coordination of this general transition in chromatin status because split clusters displayed premature H3K4me3 marks on either side of the breakpoint. Although the gain of H3K4me3 and the concurrent weakening of H3K27me3 at the mutant *Hoxd10* locus coincided with its early ectopic transcription, similar imbalances at the inverted *Hoxd11* and *Hoxd12* loci did not elicit the same transcriptional response. From this, we conclude that H3K4me3 chromatin modification is necessary but not sufficient for proper *Hox* gene transcriptional control and that remote enhancer sequences must have contributed to the maintenance of clustered organization during animal evolution.

References and Notes

1. D. Duboule, P. Dollé, *EMBO J.* **8**, 1497 (1989).
2. A. Graham, N. Papalopulu, R. Krumlauf, *Cell* **57**, 367 (1989).
3. R. Krumlauf, *Cell* **78**, 191 (1994).
4. J. C. Izpisúa-Belmonte, H. Falkenstein, P. Dollé, A. Renucci, D. Duboule, *EMBO J.* **10**, 2279 (1991).
5. D. Duboule, *Development* **134**, 2549 (2007).
6. M. Kmita, D. Duboule, *Science* **301**, 331 (2003).
7. P. Dollé, J. C. Izpisúa-Belmonte, H. Falkenstein, A. Renucci, D. Duboule, *Nature* **342**, 767 (1989).
8. T. Kondo, D. Duboule, *Cell* **97**, 407 (1999).
9. S. Chambeyron, W. A. Bickmore, *Genes Dev.* **18**, 1119 (2004).
10. Y. B. Schwartz, V. Pirrotta, *Nat. Rev. Genet.* **8**, 9 (2007).
11. J. Simon, A. Chiang, W. Bender, *Development* **114**, 493 (1992).
12. M. van Lohuizen, *Cell. Mol. Life Sci.* **54**, 71 (1998).
13. R. Cao *et al*., *Science* **298**, 1039 (2002).
14. B. Czermin *et al*., *Cell* **111**, 185 (2002).
15. A. Kuzmichev, K. Nishioka, H. Erdjument-Bromage, P. Tempst, D. Reinberg, *Genes Dev.* **16**, 2893 (2002).
16. J. Müller *et al*., *Cell* **111**, 197 (2002).
17. T. Kouzarides, *Cell* **128**, 693 (2007).
18. B. E. Bernstein *et al*., *Cell* **120**, 169 (2005).
19. A. P. Bracken, N. Dietrich, D. Pasini, K. H. Hansen, K. Helin, *Genes Dev.* **20**, 1123 (2006).
20. T. I. Lee *et al*., *Cell* **125**, 301 (2006).
21. J. L. Rinn *et al*., *Cell* **129**, 1311 (2007).
22. J. Deschamps, J. van Nes, *Development* **132**, 2931 (2005).
23. A. P. Lee, E. G. Koh, A. Tay, S. Brenner, B. Venkatesh, *Proc. Natl. Acad. Sci. U.S.A.* **103**, 6994 (2006).
24. B. E. Bernstein *et al*., *Cell* **125**, 315 (2006).
25. F. Spitz, C. Herkenne, M. A. Morris, D. Duboule, *Nat. Genet.* **37**, 889 (2005).
26. P. Tschopp, B. Tarchini, F. Spitz, J. Zakany, D. Duboule, *PLoS Genet.* **5**, e1000398 (2009).
27. T. Montavon, J. F. Le Garrec, M. Kerszberg, D. Duboule, *Genes Dev.* **22**, 346 (2008).
28. A. S. Chi, B. E. Bernstein, *Science* **323**, 220 (2009).

29. We thank T. Montavon, A. Puglisi, and D. Schübeler for advice; F. Chabaud for cell culture; and P. Descombes and members of the Genomics Platform for their help with tiling arrays. N.S. was supported by a European Molecular Biology Organization long-term fellowship. This work was funded by the University of Geneva, the Federal Institute of Technology in Lausanne, the Swiss National Research Fund, the National Research Center Frontiers in Genetics, and the European Union program Crescendo. Data and analysis are available for download from ArrayExpress (accession E-TABM-677).

Supporting Online Material

www.sciencemag.org/cgi/content/full/324/5932/1320/DC1
Materials and Methods
Figs. S1 to S3
References

27 January 2009; accepted 17 April 2009
10.1126/science.1171468

McsB Is a Protein Arginine Kinase That Phosphorylates and Inhibits the Heat-Shock Regulator CtsR

Jakob Fuhrmann,[1]* Andreas Schmidt,[2]* Silvia Spiess,[3] Anita Lehner,[1] Kürşad Turgay,[4] Karl Mechtler,[1,5] Emmanuelle Charpentier,[3,6] Tim Clausen[1]†

All living organisms face a variety of environmental stresses that cause the misfolding and aggregation of proteins. To eliminate damaged proteins, cells developed highly efficient stress response and protein quality control systems. We performed a biochemical and structural analysis of the bacterial CtsR/McsB stress response. The crystal structure of the CtsR repressor, in complex with DNA, pinpointed key residues important for high-affinity binding to the promoter regions of heat-shock genes. Moreover, biochemical characterization of McsB revealed that McsB specifically phosphorylates arginine residues in the DNA binding domain of CtsR, thereby impairing its function as a repressor of stress response genes. Identification of the CtsR/McsB arginine phospho-switch expands the repertoire of possible protein modifications involved in prokaryotic and eukaryotic transcriptional regulation.

One of the most intensely studied stress-response pathways is the bacterial heat-shock response. In the Gram-positive model organism *Bacillus subtilis*, the heat-shock response is mediated by a complex regulatory network (*1*, *2*) that is under control of at least four

major transcriptional regulators, including the alternative sigma factor σB (*3*), the two-component response regulator CssR (*4*), and the repressors HrcA (*5*) and CtsR (*6*, *7*). The latter factor, CtsR, controls the expression of genes encoding the HSP100/Clp chaperones and the protease ClpP (*6*, *8*) that constitute the core of the bacterial protein quality control system (*9*, *10*). CtsR is encoded by the first gene of the *clpC* operon that includes *ctsR*, *mcsA*, *mcsB*, and *clpC* (*6*). The dimeric repressor consists of an N-terminal domain with a helix-turn-helix (HTH) motif and a C-terminal domain of unknown function (*11*). In *B. subtilis*, CtsR represses transcription of the *clpC* heat shock operon and the *clpE* and *clpP* genes by binding specifically to a seven-nucleotide direct repeat sequence located upstream of the transcriptional start sites (*7*). Stress-induced transcription of the *clp* genes depends on the inactivation of CtsR by McsB (*12*). McsB shows pronounced homology to phosphagen kinases (PhKs) and has been reported to exhibit tyrosine kinase activity (*12*, *13*). Under normal growth conditions, McsB is captured and inhibited by ClpC. However, when bacteria are exposed to stress situations, the ClpC chaperone preferentially interacts with misfolded proteins. It is assumed that the released McsB can now form a complex with CtsR, thereby displacing it from DNA and inducing the expression of heat-shock genes (*14*). Alternatively, the phosphorylation of CtsR by McsB may be critical for the release of the repressor from DNA (*12*). To clarify and delineate the precise function of CtsR and McsB in the bacterial stress response, we screened the respective proteins from various Gram-positive bacteria for recombinant production and succeeded in reconstituting the *Bacillus stearothermophilus* CtsR/McsB system in vitro.

To uncover how McsB modulates the repressor activity of CtsR, we performed electrophoretic mobility shift assays (EMSAs) (Fig. 1A). Addition of CtsR to the 258–base pair (bp) *clpC* promoter containing three *ctsr* half sites led to a substantial band shift caused by the formation of a $CtsR_4$/DNA complex. Addition of McsB yielded two lower migrating bands that represent $CtsR_2$/DNA and free DNA. The McsB-dependent release of CtsR was observed only in the presence of Mg/adenosine triphosphate (ATP), whereas addition of EDTA or phosphatase counteracted the effect of McsB. Because no protein-protein interaction could be detected by native gel analysis or size exclusion chromatography, we speculated that McsB and CtsR interact transiently and that phosphorylation of CtsR by McsB abolishes its binding to DNA. To test this hypothesis, CtsR was incubated with McsB in the presence of ATP, and subsequently, phosphorylated CtsR (CtsR-P) was separated from nonphosphorylated CtsR by heparin affinity chromatography (Fig. 1B). Mass spectrometry (MS) analysis of CtsR-P revealed two protein species with either one or two phosphate moieties per protomer (Fig. 1B). In contrast to unmodified CtsR, the isolated CtsR-P cannot bind to its target DNA, as deduced from isothermal titration calorimetry (ITC) and gel-shift experiments (Fig. 1, C and D). Removal of the phosphate group by alkaline phosphatase fully restored the DNA binding capability of CtsR. Thus, phosphorylation of CtsR by McsB is sufficient to inhibit the repressor function of CtsR.

To understand how phosphorylation of CtsR affects DNA binding, we determined the crystal structure of CtsR bound to a 26-bp DNA derivative of the *clpC* promoter (table S1). The $CtsR_2$/DNA structure revealed that the CtsR protomer is composed of two distinct domains: (i) an N-terminal DNA binding domain that adopts the winged HTH fold (residues 2 to 72) and (ii) a C-terminal dimerization domain (residues 79 to 153) that consists of four α helices organized in a four-helix bundle (Fig. 2A). The DNA reading heads of the major and minor groove comprise the recognition helix of the HTH motif and the extended β-hairpin wing, respectively. Key residues for recognizing and binding the *ctsr* consensus sequence are indicated in Fig. 2A and fig. S3. After obtaining a molecular model of the CtsR/DNA complex, we used MS to pinpoint individual phosphorylation sites. Our initial analyses of "in-solution" and "in-gel" digested CtsR-P were not successful; thus, we attempted to sequence mono-phosphorylated CtsR in a "top-down" MS experiment (Fig. 2B). Purified CtsR-P was directly infused into the mass spectrometer and fragmented by different techniques including electron-capture dissociation (ECD), collisionally activated dissociation (CAD), and infrared multiphoton dissociation (IRMPD). Mapping of the resulting modified protein fragments to the CtsR amino acid sequence revealed that the phosphorylation sites reside in the winged HTH domain. Furthermore, the broad distribution of modified fragments pointed to the existence of product isoforms with different phosphorylation sites. The highest probability for a phosphorylation event was observed for the region

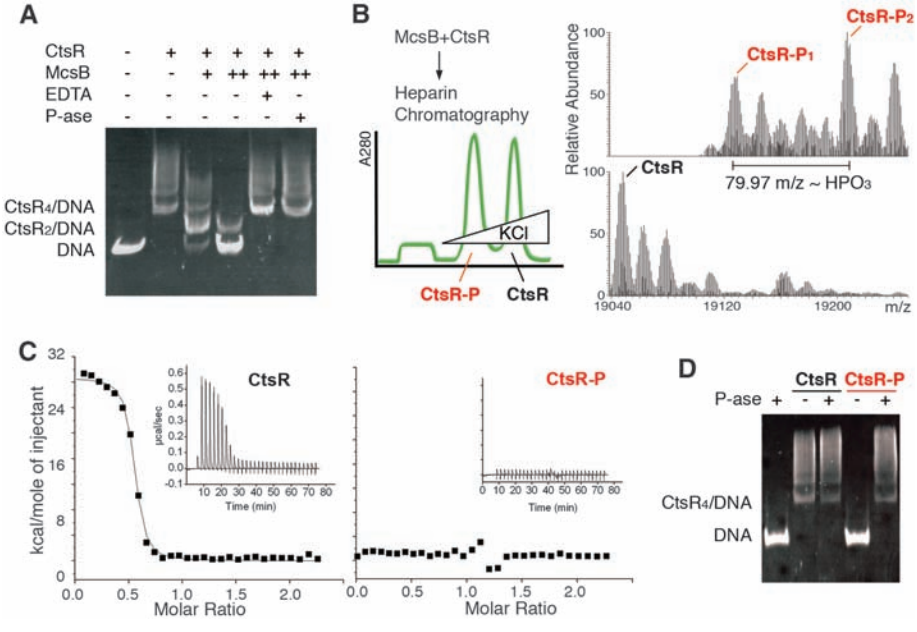

Fig. 1. Phosphorylation of CtsR impedes DNA binding. (**A**) EMSA analysis of the DNA binding capability of CtsR in the presence of McsB. CtsR was incubated with a *clpC* promoter fragment, McsB (+, 2 μM; ++, 8 μM), EDTA, and phosphatase (P-ase), as indicated. The promoter fragment, which was visualized by ethidium bromide staining of the native polyacrylamide gel, was either bound to one ($CtsR_2$/DNA) or two ($CtsR_4$/DNA) CtsR dimers. (**B**) Schematic presentation of the separation of CtsR-P from CtsR and McsB by heparin chromatography (left) and deconvoluted MS spectra of CtsR (average mass of 19047.2 daltons) and CtsR-P (19127.2 and 19207.1 daltons for mono- and di-phosphorylated isoforms, respectively) (right). (**C**) ITC analysis of $CtsR_2$/DNA complex formation. The 26-bp DNA duplex containing the *ctsr* box was injected into the sample cell containing either CtsR or CtsR-P (inset). The area under each peak was integrated and plotted against the molar ratio DNA/CtsR inside the sample cell. Thermodynamic values of CtsR/DNA complex formation are K_d = 22.2 ± 3.0 nM and n = 0.53 (reflecting the stoichiometry of bound DNA per CtsR protomer), whereas DNA binding of CtsR-P could not be detected by ITC. (**D**) EMSA analysis of the DNA binding capability of CtsR and CtsR-P, before and after phosphatase treatment.

[1]Research Institute of Molecular Pathology, Dr. Bohrgasse 7, A-1030 Vienna, Austria. [2]Christian Doppler Laboratory for Proteome Analysis, University of Vienna, Dr. Bohrgasse 3, A-1030 Vienna, Austria. [3]Max F. Perutz Laboratories, University of Vienna, Dr. Bohrgasse 9, A-1030 Vienna, Austria. [4]Institute for Biology–Microbiology, Freie Universität Berlin, Königin-Luisé-Str. 12-16, 14195 Berlin, Germany. [5]Institute for Molecular Biotechnology–IMBA, Dr. Bohrgasse 3, A-1030 Vienna, Austria. [6]The Laboratory for Molecular Infection Medicine Sweden, Umeå University, S-90187 Umeå, Sweden.

*These authors contributed equally to the work.
†To whom correspondence should be addressed. E-mail: clausen@imp.univie.ac.at

Tyr[55] to Asp[82], making up the β-hairpin wing (Fig. 2A). A lower, albeit still substantial, number of modified fragments matched the N-terminal segment from Ser[18] to Tyr[55].

To identify individual CtsR phosphorylation sites, we established a modified protocol for sample preparation and MS analysis (*15*). Most importantly, we implemented ECD and CAD fragmentation in two parallel MS/MS experiments. Only the ECD MS/MS spectrum of the phosphorylated CtsR peptide I_{57}VESKpRGGGGYIRIM$_{71}$ (*16*) allowed the unambiguous identification of Arg[62] as the site of modification (Fig. 2C). Both c- and z-fragment ion series unveiled a fragment of 236.067 daltons, reflecting the addition of a phosphate moiety (79.966 daltons) to an Arg residue (156.101 daltons). Moreover, CAD MS/MS of the I_{57}VESKpRGGGGYIRIM$_{71}$ phosphopeptide resulted in a discrete mass shift of 98 daltons, indicating the loss of phosphoric acid (fig. S1). This fragmentation behavior argues against a tyrosine kinase activity of McsB because phospho-tyrosine is stable upon CAD fragmentation (*17*). Further MS analysis led to the identification of two additional phosphorylation sites, Arg[28] and Arg[49] (fig. S2). Consistent with the results of the top-down approach, these amino acids are located within the winged HTH domain. Moreover, all Arg residues are strictly conserved in the CtsR protein family and play a crucial role in DNA binding, as predicted by our crystal structure. Arg[62] is a residue within the β wing and deeply invades the minor groove of the DNA duplex. In addition to undergoing extensive van der Waals contacts, the guanidinium group of Arg[62] forms hydrogen bonds with the DNA backbone and with one of the thymine pyrimidine carbonyls (Fig. 2A). Similarly, in the major groove of the CtsR consensus site, Arg[28] and Arg[49] bind to purine bases and coordinate the sugar-phosphate backbone, respectively (fig. S3).

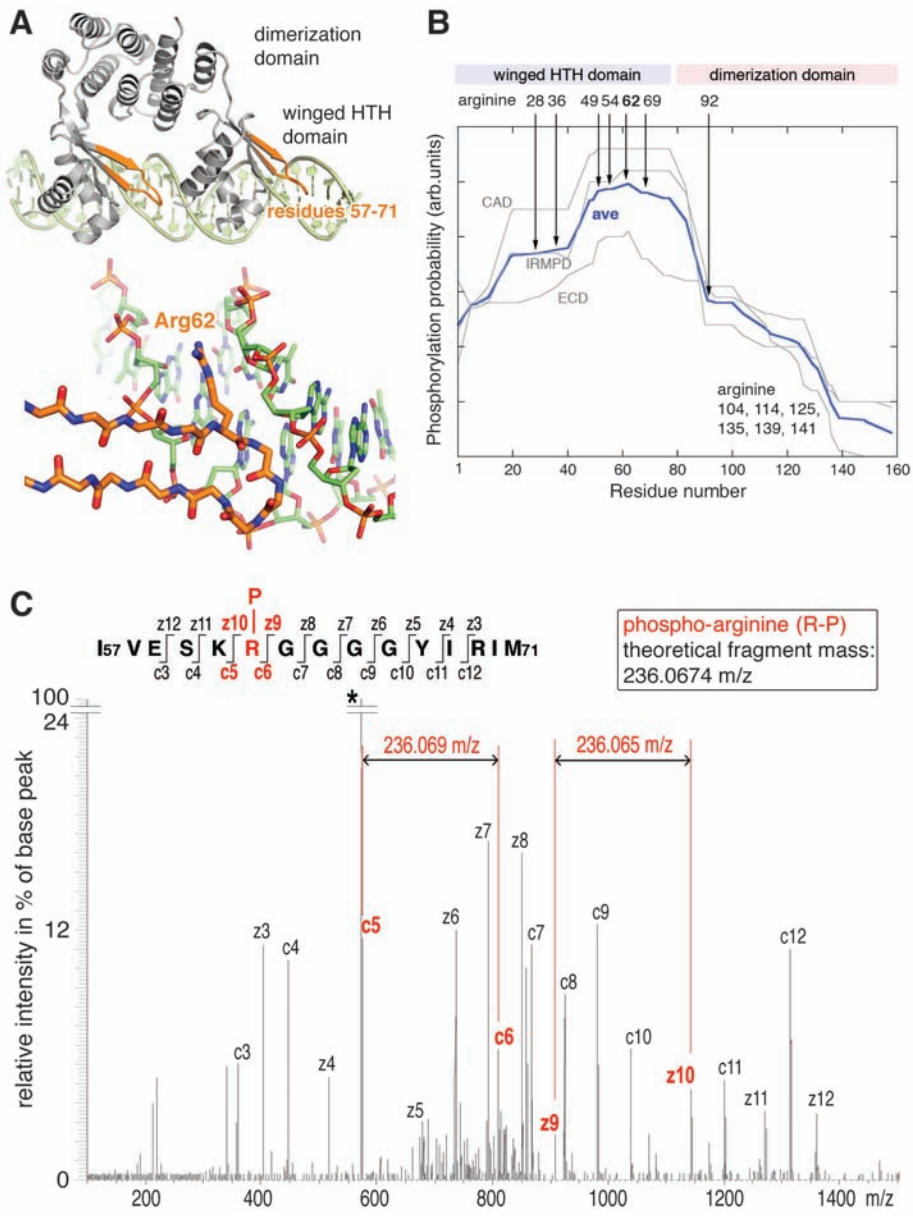

Fig. 2. Identification of arginine phosphorylation sites of CtsR. (**A**) Ribbon diagram showing the CtsR dimer (gray, with labeled domains) bound to the DNA direct repeat motif (green). The identified CtsR phosphopeptide I_{57}VESKpRGGGGYIRIM$_{71}$, which constitutes the β-hairpin of the winged HTH domain penetrating the DNA minor groove, is highlighted in orange. The lower panel illustrates the binding mode of Arg[62] (orange), the main phosphorylation site, at the floor of the DNA minor groove (green). (**B**) Phosphosite mapping with top-down MS. The mono-phosphorylated isoform of full-length CtsR was sequenced by three different fragmentation techniques. The blue line represents the average (ave) value of the three experimental setups and refers to the number of fragments additionally identified in CtsR-P, relative to unmodified CtsR. The residue with the highest phosphorylation score was Arg[62]. (**C**) ECD-MS/MS spectrum of the major phosphopeptide I_{57}VESKpRGGGGYIRIM$_{71}$ obtained after chymotryptic cleavage of phosphorylated CtsR. Individual fragments are labeled according to the c- or z-ion nomenclature. The characteristic mass difference of the phosphorylated Arg[62] is highlighted, and the threefold charged precursor ion is marked with an asterisk. m/z, mass/charge ratio.

To explore the functional relevance of the identified phosphosites, we conducted a mutational analysis of full-length CtsR by introducing various Arg-to-Lys mutations. Mutating the target sites in position 28, 49, and 62 (3RK) did not completely abolish, but did substantially reduce the phosphorylation of CtsR by McsB (Fig. 3A). Moreover, a mutant protein (8RK), in which the eight Arg residues located in the DNA binding region were replaced by Lys residues, was completely unsusceptible to McsB modification. Reintroduction of Arg[62] (7RK) markedly restored the phosphorylation potential. To study the direct effect of CtsR phosphorylation on DNA binding, we replaced Arg[62] by a phosphomimicking Glu residue. EMSA experiments clearly demonstrated that the Arg[62] → Glu[62] (R62E) mutant lost its capability to bind DNA (Fig. 3B), thus corroborating our finding that phosphorylation of CtsR alone is sufficient to inhibit its repressor activity. Conversely, replacing Arg[62] by Lys[62] did not alter the DNA binding ability of CtsR in band-shift assays. To test which state of CtsR is targeted by McsB, we incubated the kinase with DNA-bound and -unbound CtsR. Following the interaction with DNA over time revealed that McsB preferentially phosphorylates free CtsR, thereby preventing DNA complex formation (fig. S4). We conclude that the selective introduction of a negatively charged phosphate moiety functions as a molecular switch regulating DNA binding. Whereas the unphosphorylated CtsR binds with high affinity to its DNA consensus site and inhibits transcription of downstream genes, the McsB-phosphorylated CtsR repressor is not able to bind to DNA, thus allowing heat-shock gene expression.

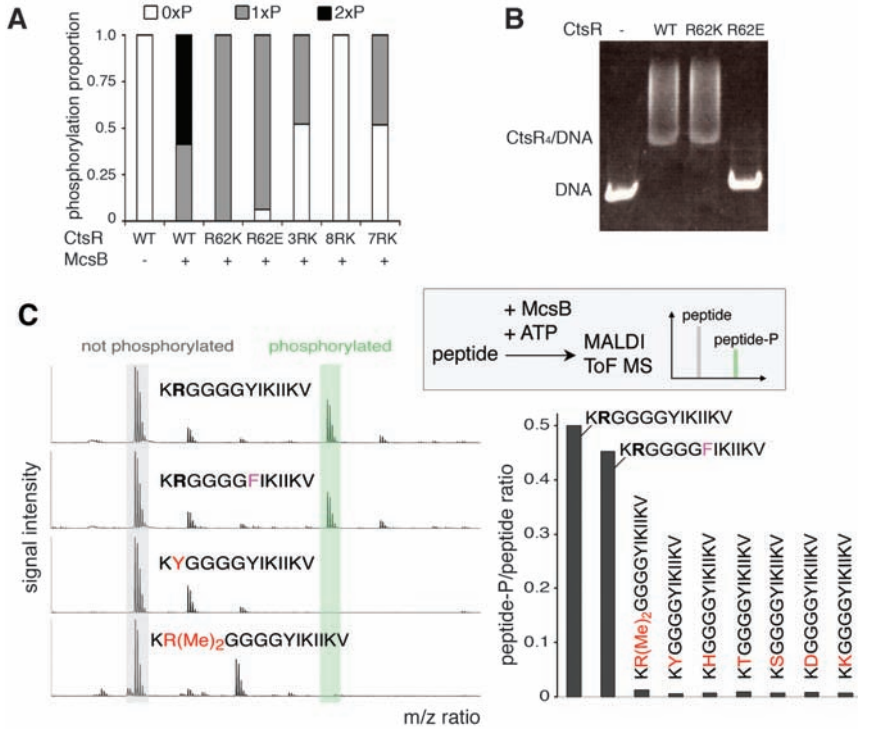

Fig. 3. Characterization of McsB-mediated arginine phosphorylation. (**A**) Phosphorylation level of CtsR Arg mutants analyzed by electrospray ionization–MS. The Arg-to-Lys mutants are 28/49/62 (3RK), 28/36/49/54/62/69/114/125 (8RK), and 28/36/49/54/69/114/125 (7RK). (**B**) DNA binding ability of different CtsR mutants in gel-shift assays. (**C**) Peptide phosphorylation assay (schematically shown in the inset). (Left) Matrix-assisted laser desorption/ionization–time-of-flight spectra of selected peptides after incubation with McsB. Non-phosphorylated and phosphorylated peptides are marked in gray and green, respectively. (Right) Effect of the exchange of Arg to other potential phospho-acceptor sites (shown in red) on the phosphorylation efficiency.

To verify our finding that McsB is a protein arginine kinase, we established an in vitro phosphorylation assay (Fig. 3C) using synthetic oligopeptides that resembled the CtsR sequence (residues 61 to 73). To avoid side effects during sample preparation that would preclude quantification of the phosphorylation reaction, we replaced one potential oxidation site (Met^{71}) and one arginine (Arg^{69}), yielding the 13-residue model substrate K_{61}RGGGGYIKIIKV$_{73}$. Systematic incorporation of potential phosphorylation sites (Tyr, Ser, Thr, His, Asp, and Lys) in position 62 revealed that only peptides with an Arg moiety are modified by McsB (Fig. 3C). Moreover, modification of the guanidinium group of Arg^{62} by asymmetric dimethylation prevented McsB-mediated modification. Additionally, we analyzed the purified phosphopeptide K_{61}RGGGGYIKIIKV$_{73}$ by ^{31}P nuclear magnetic resonance (NMR) spectroscopy (fig. S5). The chemical shift of about –2.4 parts per million (ppm) fits well to the measured NMR spectrum of free phospho-arginine (–3.0 ppm) (*18*), suggesting that the phosphate is attached via a phosphoramidate N-P linkage. Corresponding spectra of O-P linked phosphor compounds (as, for example, phospho-tyrosine, -serine, and -threonine) exhibit markedly higher chemical shifts of ~0.7 to 4.0 ppm (*18*). Thus, McsB is a protein kinase that acts exclusively on Arg residues, phosphorylating one of the amine nitrogens of the guanidinium group.

Phosphorylation of the free amino acid L-arginine by eukaryotic PhKs yields a chemically labile compound (*19*). We studied the CtsR/McsB system of a thermophilic organism living at ~55°C and thus explored the thermostability of a phosphorylated Arg residue present in a peptide context. For this purpose, we phosphorylated the K_{61}RGGGGYIKIIKV$_{73}$ peptide with McsB, incubated the purified phosphopeptide at different temperatures, and quantified the stability of the phosphorylation signal by high-performance liquid chromatography–MS analysis. The results clearly showed that peptide arginine phosphorylation is surprisingly stable up to 60°C. Dephosphorylation of the phosphopeptide occurred only at 95°C, with a half life $t_{1/2}$ of ~130 min (fig. S6). Therefore, phosphorylation of protein arginine residues should represent a relevant biological signal.

Sequence analysis indicated that the McsB protein arginine kinase exhibits no substantial homology to known Ser, Thr, Tyr, or His kinases. However, the catalytic domain of McsB is highly homologous to the catalytic domain of PhKs (*12*, *13*), which are involved in maintaining energy homeostasis but not in intermolecular signaling (*20*). Mutational analyses revealed that McsB and PhKs use a common mechanism to phosphorylate the terminal guanidinium group of substrates (fig. S7) (*14*). However, in contrast to PhKs where substrate specificity is primarily determined by the N-terminal domain, McsB harbors a distinct C-terminal domain that may redirect the substrate specificity from free Arg to protein-incorporated Arg residues.

McsB appears to be the founding member of a new class of protein kinases acting specifically on Arg residues. It should be noted that protein arginine phosphorylation has been reported previously (*21*). Remarkably, histone H3 was identified as a potential eukaryotic target (*22*), implying that Arg phosphorylation activity might be relevant for epigenetic regulation. However, these analyses failed to identify the corresponding kinase and obtained only indirect evidence for Arg modification. The thorough characterization of a protein arginine kinase presented in this work should provide the experimental tools to directly address the impact of Arg phosphorylation in prokaryotic and eukaryotic signaling pathways.

References and Notes

1. M. Hecker, W. Schumann, U. Volker, *Mol. Microbiol.* **19**, 417 (1996).
2. W. Schumann, M. Hecker, T. Msadek, in *Bacillus subtilis and Its Closest Relatives: From Genes to Cells*, A. L. Sonenshein, J. A. Hoch, R. Losick, Eds. (American Society for Microbiology Press, Washington, DC, 2002).
3. W. G. Haldenwang, R. Losick, *Nature* **282**, 256 (1979).
4. H. L. Hyyrylainen *et al.*, *Mol. Microbiol.* **41**, 1159 (2001).
5. A. Schulz, W. Schumann, *J. Bacteriol.* **178**, 1088 (1996).
6. E. Kruger, M. Hecker, *J. Bacteriol.* **180**, 6681 (1998).
7. I. Derre, G. Rapoport, T. Msadek, *Mol. Microbiol.* **31**, 117 (1999).
8. I. Derre, G. Rapoport, K. Devine, M. Rose, T. Msadek, *Mol. Microbiol.* **32**, 581 (1999).
9. S. Wickner, M. R. Maurizi, S. Gottesman, *Science* **286**, 1888 (1999).
10. R. T. Sauer *et al.*, *Cell* **119**, 9 (2004).
11. I. Derre, G. Rapoport, T. Msadek, *Mol. Microbiol.* **38**, 335 (2000).
12. E. Kruger, D. Zuhlke, E. Witt, H. Ludwig, M. Hecker, *EMBO J.* **20**, 852 (2001).
13. J. Kirstein, K. Turgay, *J. Mol. Microbiol. Biotechnol.* **9**, 182 (2005).
14. J. Kirstein, D. Zuhlke, U. Gerth, K. Turgay, M. Hecker, *EMBO J.* **24**, 3435 (2005).
15. Materials and methods are available as supporting material on *Science* Online. A detailed description of the MS approach is provided.
16. Single-letter abbreviations for the amino acid residues are as follows: A, Ala; C, Cys; D, Asp; E, Glu; F, Phe; G, Gly; H, His; I, Ile; K, Lys; L, Leu; M, Met; N, Asn; P, Pro; Q, Gln; R, Arg; S, Ser; T, Thr; V, Val; W, Trp; and Y, Tyr.
17. A. Tholey, J. Reed, W. D. Lehmann, *J. Mass Spectrom.* **34**, 117 (1999).
18. T. L. James, *CRC Crit. Rev. Biochem.* **18**, 1 (1985).
19. A. Sickmann, H. E. Meyer, *Proteomics* **1**, 200 (2001).
20. W. R. Ellington, *Annu. Rev. Physiol.* **63**, 289 (2001).
21. H. R. Matthews, *Pharmacol. Ther.* **67**, 323 (1995).
22. B. T. Wakim, G. D. Aswad, *J. Biol. Chem.* **269**, 2722 (1994).

23. We thank D. Fiegen and D. Reinert (Boehringer Ingelheim) and the staff at Swiss Light Source for assistance with collecting synchrotron data, A. Carrieri for his contribution with the kinase assays, L. Becker for the NMR analysis of phosphopeptides, T. Krojer and D. Hellerschmied for their support in the structural analysis of CtsR, and C. Stingl and M. Mazanek for assisting MS analysis. The Research Institute of Molecular Pathology is funded by

Boehringer Ingelheim. J.F., S.S., E.C., and T.C. were supported by Wiener Wissenschafts, Forschungs und Technologiefonds; A.S. by the Christian-Doppler-Society; K.T. by the Deutsche Forschungsgemeinschaft; and T.C. by the European Molecular Biology Organization Young Investigator Program. This work was further supported by the Austrian Proteomics Platform (GEN-AU). The Protein Data Bank accession number for the $CtsR_2$/DNA complex is 3H0D.

Supporting Online Material
www.sciencemag.org/cgi/content/full/324/5932/1323/DC1
Materials and Methods
Figs. S1 to S8
Table S1
References

22 December 2008; accepted 13 April 2009
10.1126/science.1170088

Rhes, a Striatal Specific Protein, Mediates Mutant-Huntingtin Cytotoxicity

Srinivasa Subramaniam, Katherine M. Sixt, Roxanne Barrow, Solomon H. Snyder*

Huntington's disease (HD) is caused by a polyglutamine repeat in the protein huntingtin (Htt) with mutant Htt (mHtt) expressed throughout the body and similarly in all brain regions. Yet, HD neuropathology is largely restricted to the corpus striatum. We report that the small guanine nucleotide–binding protein Rhes, which is localized very selectively to the striatum, binds physiologically to mHtt. Using cultured cells, we found Rhes induces sumoylation of mHtt, which leads to cytotoxicity. Thus, Rhes-mHtt interactions can account for the localized neuropathology of HD.

Huntington's disease (HD), a genetically dominant neurodegenerative disorder, reflects expansion of a polyglutamine repeat in the protein huntingtin (Htt) (*1*). Mutant Htt (mHtt) occurs uniformly throughout the brain and peripheral tissues. Yet, HD is brain-specific with profound abnormal movements related to selective, gross degeneration of the corpus striatum and lesser damage to the cerebral cortex eliciting dementia (*2*, *3*). Molecular mechanisms causing mHtt cytotoxicity are unclear. mHtt forms protein aggregates, which may be neuroprotective with soluble mHtt linked to cytotoxicity (*4*–*7*). mHtt is sumoylated, which increases the soluble form of mHtt and elicits cytotoxicity and neurotoxicity in a *Drosophila* model of HD (*8*).

Rhes (Ras homolog enriched in striatum) is a small guanine nucleotide–binding protein (G protein) very selectively localized to the striatum (*9*). To determine whether Rhes binds to Htt, we overexpressed Rhes in HEK293 cells where it bound to both wild-type (wt) Htt and mHtt (Fig. 1A) (*10*). In conditionally immortalized Htt knock-in striatal neuronal cells (*11*), which lack endogenous Rhes (fig. S1C), overexpressed Rhes bound robustly to endogenous mHtt (Fig. 1B). In HD transgenic mice (*12*), endogenous striatal mHtt coprecipitated with Rhes (Fig. 1C). In the presence of purified Rhes and Htt, Rhes bound much more to mHtt than wtHtt protein (fig. S1A). Rhes did not bind to ataxin (fig. S1B), a polyglutamine-repeat protein involved in another neurodegenerative disorder, spinocerebellar ataxia.

To ascertain whether Rhes influences mHtt cytotoxicity, we used several cell lines. In

The Solomon H. Snyder Department of Neuroscience, Johns Hopkins University School of Medicine, 725 North Wolfe Street, Baltimore, MD 21205, USA.

*To whom correspondence should be addressed. E-mail: ssnyder@jhmi.edu

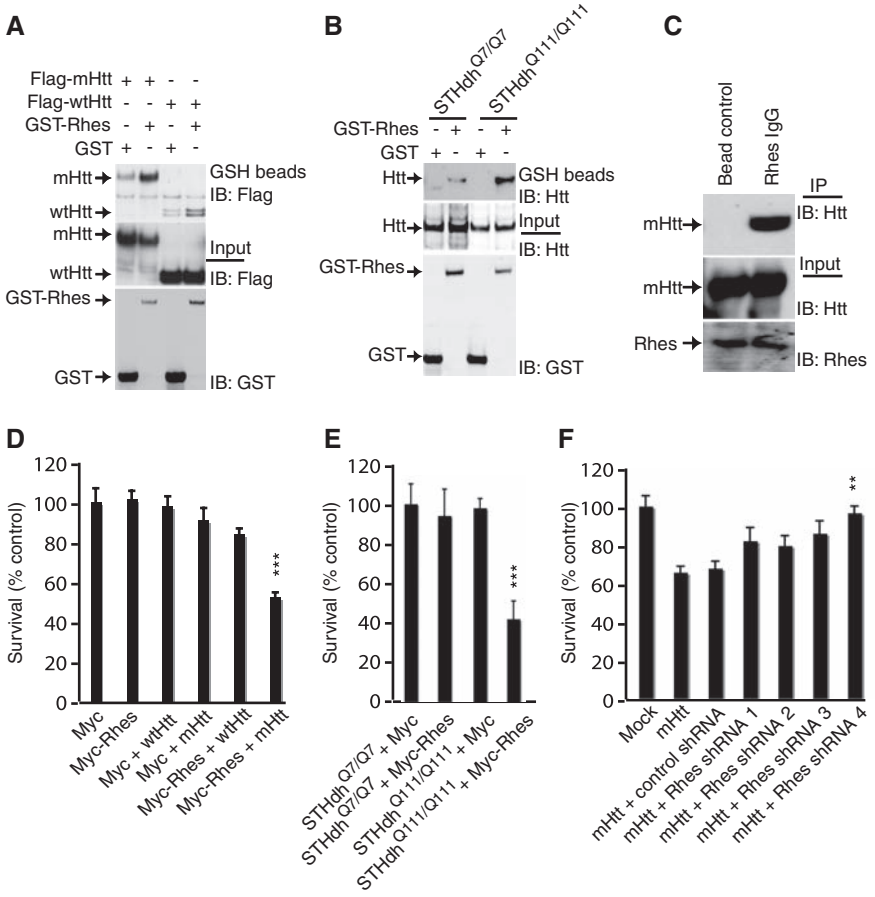

Fig. 1. Rhes binds Htt and affects cell survival. (**A**) Rhes interacts with N-terminal Htt. HEK293 cells were transfected with glutathione *S*-transferase (GST) or GST-Rhes together with Flag-tagged Htt or the N-terminal fragment containing 171 amino acids and 18 glutamines (wtHtt) or 82 glutamines (mHtt). After 48 hours, cell lysates were glutathione (GSH) precipitated and immunoblotted (IB) for Flag. (**B**) Rhes interacts with full-length Htt. Striatal cells expressing wild-type Htt ($STHdh^{Q7/Q7}$) or mutant Htt ($STHdh^{Q111/Q111}$) were transfected with GST or GST-Rhes. After 48 hours, cell lysates were GSH-precipitated and immunoblotted for Htt. Htt and GST inputs are shown. (**C**) Rhes interacts with mHtt in striatum. Striatum of transgenic mice expressing mHtt was lysed and immunoprecipitated with Rhes antibody or immunoglobulin IgG alone (bead control). Immunoprecipitates were probed with an N-terminal–specific Htt antibody (N-Htt). (**D**) Rhes reduces cell survival. HEK293 cells were transfected with Myc/Myc-Rhes and wtHtt–mHtt constructs. ***P < 0.005 versus mHtt alone. (**E**) Wild-type ($STHdh^{Q7/Q7}$) or mutant ($STHdh^{Q111/Q111}$) striatal cells were transfected with Myc/Myc-Rhes. ***P < 0.005 versus Myc. (**F**) Depletion of Rhes prevents PC12 cell death. Control short hairpin–mediated (shRNA) or Rhes shRNA 1 to 4 were cotransfected with mHtt. Only shRNA4 was significantly cytoprotective (**P < 0.01 versus control shRNA). After 48 hours, cell survival was measured by MTT.